Jo-Young Suh
Oh-Cheol Jeung
Byung-Ju Choi
Jin-Woo Park

Effects of a novel calcium titanate coating on the osseointegration of blasted endosseous implants in rabbit tibiae

Authors' affiliations:
Jo-Young Suh, Oh-Cheol Jeung, Jin-Woo Park, Department of Periodontology, College of Dentistry, Kyungpook National University, Daegu, South Korea
Byung-Ju Choi, Department of Dental Pharmacology, College of Dentistry, Kyungpook National University, Daegu, South Korea

Correspondence to:
Professor Jin-Woo Park
Department of Periodontology
College of Dentistry
Kyungpook National University
188-1, Samduk 2Ga, Jung-Gu, Daegu 700-412
South Korea
Tel.: +82 53 660 6913
Fax: +82 53 427 3263
e-mail: jinwoo@mail.knu.ac.kr

Date:
Accepted 20 April 2006

To cite this article:
Suh J-Y, Jeung O-C, Choi B-J, Park J-W. Effects of a novel calcium titanate coating on the osseointegration of blasted endosseous implants in rabbit tibiae.
Clin. Oral Impl. Res. **18**, 2007; 362–369
doi: 10.1111/j.1600-0501.2006.01323.x

Key words: calcium titanate coating, hydroxyapatite blasting, osseointegration, rabbit tibia, titanium implant

Abstract

Objective: The purpose of this study was to investigate the effects of a nanostructured calcium coating on the surfaces of blasted Ti implants on peri-implant bone formation in the rabbit tibiae.

Material and methods: Threaded implants (3.75 mm in diameter, 6 mm in length) were roughened by hydroxyapatite (HA) blasting (control; blasted implants). The implants were then hydrothermally treated in a Ca-containing solution for 24 h to prepare Ca-incorporated Ti surfaces (experimental; blasted/Ca implants). Surface characterizations were performed by scanning electron microscopy and stylus profilometry before and after Ca coating. Forty-two implants (21 control and 21 experimental) were placed in the proximal tibiae of seven New Zealand White rabbits. Each rabbit received six implants. To evaluate the effects of the nanostructured Ca coating on the peri-implant bone-healing response, removal torque tests and histomorphometric analyses were performed 6 weeks after surgery.

Results: The Ca coating did not significantly change the surface properties produced by blasting at the micron level. Histologically, active bone apposition was observed in the blasted/Ca implants in the marrow space. Compared with the blasted implants, the blasted/Ca implants showed significantly increased bone-to-implant contact over the total implant length ($P<0.01$) and greater mean removal torque values ($P<0.05$).

Discussion and conclusion: The nanostructured, Ca-incorporated surface significantly enhanced the peri-implant bone-healing response of HA-blasted Ti implants. It may be concluded that the use of nanostructured, Ca-coated surfaces may have synergic effects in enhancing osseointegration of blasted Ti implants due to their micron-scaled surface properties and biologically active surface chemistry.

The predictability and long-term success rates of dental endosseous implants have been well documented (Adell et al. 1990; van Steenberghe et al. 1990); however, high implant failure rates have been reported in areas of poor quality bone such as in the posterior maxilla (Jaffin & Berman 1991). It is well known that long-term success is greatly affected by local bone conditions, such as bone quality and quantity. Today, with their rough surfaces, implants have achieved high success rates in poor bone by enhancing osseointegration via increasing bone-to-implant contact compared with implants with smooth surfaces (Wennerberg et al. 1998; Trisi et al.

1999; Khang et al. 2001; Cochran et al. 2002; Stach & Kohles 2003; Glauser et al. 2005).

Numerous approaches have been tried in order to improve clinical results with poor local bone conditions and to shorten healing periods. Many trials have focused on providing enhanced osseous stability by improving the quality of early biological events at the bone–implant interface. It is well known that microroughness and an increase in the implant surface area produced by blasting and/or acid etching enhance biomechanical bonding by optimizing the biological response of the bone and micromechanical interlocking (Davies 1998; Lossdorfer et al. 2004; Szmukler-Moncler et al. 2004a).

One of the strategies used to improve osseointegration is to make the bioinert surfaces of metallic implants bioactive, thereby favoring bone–tissue reactions at the interface. Titanium (Ti) induces osseointegration and as such it is not bioactive. Titanium is generally considered to be bioinert and not likely to form direct bonds with bone, so various kinds of bioactive materials have been coated onto the surfaces of Ti implants in order to provide optimal surface reactivity. Hydroxyapatite (HA) plasma spraying is the most frequently used coating method to produce potentially bioactive implant surfaces, but several problems, such as delamination and unpredictable biodegradation, have been reported (Hanisch et al. 1997; Albrektsson 1998; Morscher et al. 1998).

Recently, many studies have demonstrated the advantages of Ti implants incorporating calcium ions in enhancing osseointegration. Sul (2003) reported that Calcium-deposited Ti implants produced by micro-arc oxidation achieved biochemical bone bonding in an animal study. Several studies have reported that an increased calcium (Ca) composition in the outer oxide layer affected increased cell adhesion by increasing protein adsorption onto Ti surfaces at physiologic pH (Ellingsen 1991; Klinger et al. 1997). Webster et al. (2003) reported that calcium titanate ($CaTiO_3$) promoted osteoblast adhesion, and suggested $CaTiO_3$ as a strong candidate for increasing osseointegration. They confirmed the formation of $CaTiO_3$ on the surfaces of Ti-coated HA discs annealed in air. To deposit $CaTiO_3$ coatings on Ti substrates, several studies have been reported so far, such as hydrothermal treatment, hydrothermal – electrochemical treatment (Yoshimura et al. 1995; Fujishiro et al. 1998), and sol–gel coating (Kaciulis et al. 1998; Manso et al. 2003). However, those methods seem difficult to apply to Ti implants with microroughened surfaces without alteration of micron-scale surface properties including microarchitectures and surface microroughness, because of their thickness (4 – 50 μm) and the size of $CaTiO_3$ crystals (1 – 10 μm) in the coatings.

Most recently, we revealed the possibility of a novel nanostructured Ca coating of Ti implants preserving the original micron-scale topography, related to biomechanical interlocking with bone tissue, as an effective surface modification method for improving osseointegration (submitted, 2007). We were able to observe the formation of crystalline $CaTiO_3$ coating with nanometer dimension (approximately 100 nm or less in size) on Ti substrates, without alteration of surface microstructure at the micron-scale level, by controlling the reaction parameters during hydrothermal treatment. We expect that this nanostructured Ca coating of Ti implants may have advantages over other coating methods such as HA plasma spraying to confer bioactivity to Ti implants without the thick layers common with HA coating. Based on the results of earlier studies, which reported enhanced bone formation on calcium phosphate-coated surfaces of implants when compared with commercially pure titanium surfaces (Caulier et al. 1997; Karabuda et al. 1999), the bioactive surface chemistry of the Ca may provide potential synergic effects for peri-implant bone formation around endosseous Ti implants beyond the effects of the microscale surface topography.

The purpose of this study was to investigate the effects of a nanostructured Ca coating on the surfaces of Ti implants on peri-implant bone formation in the rabbit tibiae. Additionally, we investigated the effects of micron-scaled surface properties of implants in relation to biomechanical interlocking and bioactive chemical composition, and biochemical bonding with bone tissue on osseointegration of titanium implants.

For this purpose, nanostructured Ca-coated blasted implants were prepared using a hydrothermal method. Surface characterizations were performed to determine whether altered micron-scaled surface properties, including changes in surface roughness due to coating procedures, affect the corresponding results. Peri-implant bone responses were evaluated by removal torque testing and histological and histomorphometric evaluations after 6 weeks of implantation in rabbit tibiae.

Material and methods

Titanium implants and calcium coating

Screw-type implants ($n = 48$) with an external diameter of 3.75 mm and a length of 6 mm were turned from commercially pure titanium rods (ASTM Grade 2) and the surfaces were roughened by hydroxyapatite blasting. Implants roughened with hydroxyapatite particles were used in this study to obviate surface contamination resulting from blasting processes using alumina particles (MegaGen Co. Ltd., Kyungsan, Korea; Szmukler-Moncler et al. 2004b). The implants were then passivated in nitric acid according to ASTM specification F-86 (blasted implant). The Ca-coated implants were prepared using hydrothermal treatment according to our previous study (submitted, 2007) (blasted/Ca implants). Briefly, Ti implants were treated in a Ca-containing solution – a mixed solution of 0.2 M NaOH and 2 mM CaO (Sigma Chemical Co., St. Louis, MO, USA) dissolved in deionized water (Milli-Q Ultra-Pure, Millipore, Billerica, MA, USA) – using a Teflon-lined hydrothermal reactor system (ILSHIN Autoclave Co., Ltd., Daejeon, Korea) at 180°C for 24 h under a water vapor pressure of 1 MPa. We used these reaction parameters in order to preserve surface microstructure because the surface structure demonstrated relatively smooth features at a more higher pressure; the thickness of the $CaTiO_3$ coating increased on increasing the concentration of NaOH in our previous study. After treatment, Ti implants were ultrasonically cleaned in deionized water for 2 × 5 min and then air-dried for 24 h. In this study, two groups of implants were used: blasted implants as the control, and blasted/Ca implants as the experimental group. All implants were sterilized by gamma irradiation before use. To evaluate the crystalline structure and

chemical composition of the Ti oxides after surface treatment, rectangular Ti samples (20 × 10 × 1 mm) were treated in the manner described above.

Surface characterization

The experimental and control implants were subjected to surface analysis. Surface morphology was observed by scanning electron microscope (SEM; S-4200; Hitachi, Tokyo, Japan) to evaluate the micron-scaled surface structure before and after the Ca-coating procedure. Implant surface roughness measurement was performed by stylus profilometry (Form Talysurf Series 2; Taylor Hobson, London, UK). Two of each implant were measured, and three measurements were performed on each implant. All measurements were performed at the lateral flat surface of the lower part of the implants. The crystalline structure was evaluated by thin-film X-ray diffractometry (XRD, X'Pert-APD; Philips, the Netherlands), and the surface chemical compositions of coating were analyzed by X-ray photoelectron spectroscopy (XPS, MT 500/1; VG Microtech Inc., UK) and Auger electron spectroscopy (AES, PHI 680 Auger Nanoprobe; Physical Electronics, USA) using rectangular Ti samples.

Animals and surgical procedure

Seven adult male New Zealand White rabbits weighing 3–3.5 kg were used in this study. This experiment was approved by the Institutional Animal Care and Use Committee of Kyungpook National University Hospital, Daegu, Korea.

General anesthesia was induced by intramuscular injection of a combination of 1.3 ml of ketamine (100 mg/ml) (Ketara; Yuhan, Seoul, Korea) and 0.2 ml of xylazine (7 mg/kg body weight; Rompun; Bayer Korea, Seoul, Korea). The medial surfaces of proximal tibiae were used as the surgical sites. The surgical areas were shaved and the skin was washed with a mixture of iodine and 70% ethanol before surgical draping. Local anesthesia with 1 ml of 2% lidocaine (1 : 100,000 epinephrine; Yuhan, Seoul, Korea) was administered to control bleeding and to provide additional local anesthesia. Surgical sites were exposed with an incision through the skin, fascia, and periosteum at the medial surface of proximal tibiae using sterile surgical techniques.

The implant site osteotomies were prepared in the usual manner. A final drill diameter of 3 mm was used. All drilling procedures were carried out under profuse sterile saline irrigation. Six screw-shaped implants were placed in one animal; a set of three control implants and a set of three experimental implants were randomly placed in the right and left rabbit tibiae. Blasted/Ca experimental implants ($n = 21$) and blasted control implants ($n = 21$) were inserted with self-tapping. All implants penetrated the first bone cortex only.

After surgery, surgical sites were closed in layers and sutured using Vicryl (Ethicon, Somerville, NJ, USA). Antibiotics (Baytril; Bayer Korea) and analgesics (Nobin; Bayer Korea) were injected intramuscularly for 3 days to prevent postsurgical infection and to control pain. The animals were killed by intravenous injection of air 6 weeks after surgery and tissues were taken for removal torque tests and histomorphometric evaluation.

Removal torque tests

Removal torque tests were performed to evaluate implant stability in the bone bed. The removal torque value in Newton centimeter (N cm) reflects the interfacial shear strength (Johansson et al. 1998). Two of the distal implants from each leg were subjected to removal torque testing (seven rabbits; blasted/Ca experimental implants, $n = 14$; blasted control implants, $n = 14$). The implants were surgically exposed and implant removal mounts were securely connected. The leg was stabilized and the peak removal torque force was measured using a digital torque meter (MG series; Mark-10 Corporation, New York, NY, USA) with a measuring range of 0–135 N cm. A single blinded examiner recorded measurements of peak torque to initiate reverse rotation.

Surface analysis of the torqued implants

After removal torque tests, the implants were completely removed from the tibiae and were ultrasonically cleaned in 5% sodium hypochlorite solution for 10 min in order to remove the soft tissue and the nonattached bone. The implants were fixed in 4% neutral-buffered formaldehyde, dehydrated using ascending series of alcohols, and dried. The surface color of torqued implants was examined by optical inspection, and the surfaces of implants were observed by SEM for failure analysis.

Specimen preparation and histomorphometric evaluation

The most proximal implant in each leg was selected for histomorphometric evaluation. The proximal tibiae containing the implants were removed *en bloc*, fixed in 4% neutral-buffered formaldehyde, dehydrated using an ascending series of alcohols, and embedded in methyl methacrylate for undecalcified sectioning. Undecalcified cut-and-ground sections containing the central part of the implants were produced at a final thickness of 20 μm using a Macro cutting and grinding system (Exakt 310 CP series; Exakt Apparatebau, Norderstedt, Germany). The sections were stained with toluidine blue, and histomorphometric analysis was carried out using a light microscope (Axioplan 2; Carl Zeiss, Oberkochen, Germany) with an image analysis system (i-Solution, iMTechnology Inc., Daejeon, Korea) under 50 × magnification. The image was captured using a digital camera (AxioCam MRc 5; Carl Zeiss) attached to the microscope and displayed on a computer monitor. The percentage of bone-to-implant contact (BIC%) in the first three threads and the percentage of bone area inside the same threads were measured (seven rabbits; blasted/Ca experimental implants, $n = 7$; blasted control implants, $n = 7$). BIC% was measured as the percentage of the length of bone in direct contact with the implant surface. We evaluated BIC% and bone area in the first three threads because the lower parts of the implants were surrounded by the marrow space, in which bony structures are almost absent. Additionally, the BIC% in the total length of the implant except the apical part was measured. This is a useful parameter in evaluating the osteoconductivity of the implants, especially in the marrow region.

Statistical analysis

The surface roughness value, removal torque value, and histomorphometric data were processed with the SAS statistical system. The significance of the differences between the two groups was analyzed using Student's *t*-test. *P*-values less than 0.05 were considered to be statistically significant.

Results

Surface characteristics

SEM observation showed no micron-scale morphological differences between the surfaces of blasted implants and blasted/Ca implants at a magnification of × 1000 (Fig. 1a, c). Typical irregular indentations produced by blasting were observed on the surfaces of both groups of implants. However, at a relatively higher magnification (× 30,000), nanostructure formation was observed on the surface of the blasted/Ca implants (Fig. 1d). The XRD analysis of the blasted/Ca samples exhibited a set of peaks of reflection from $CaTiO_3$ (JCPDS #22-0153; Fig. 2). The blasted surfaces consisted primarily of Ti and O. Carbon was detected as a surface contaminant in the XPS survey spectra; no traces of Ca in the surfaces of blasted samples were detected. AES depth profiles showed a graded surface structure of a Ca-incorporated Ti oxide layer of the blasted/Ca samples; the relative atomic concentration of Ca was approximately 40% at the outermost surface (Fig. 3). Based on profilometry, the mean values of the roughness parameters of the blasted/Ca implant surfaces were slightly lower than those of the blasted implants ($P<0.05$; Table 1).

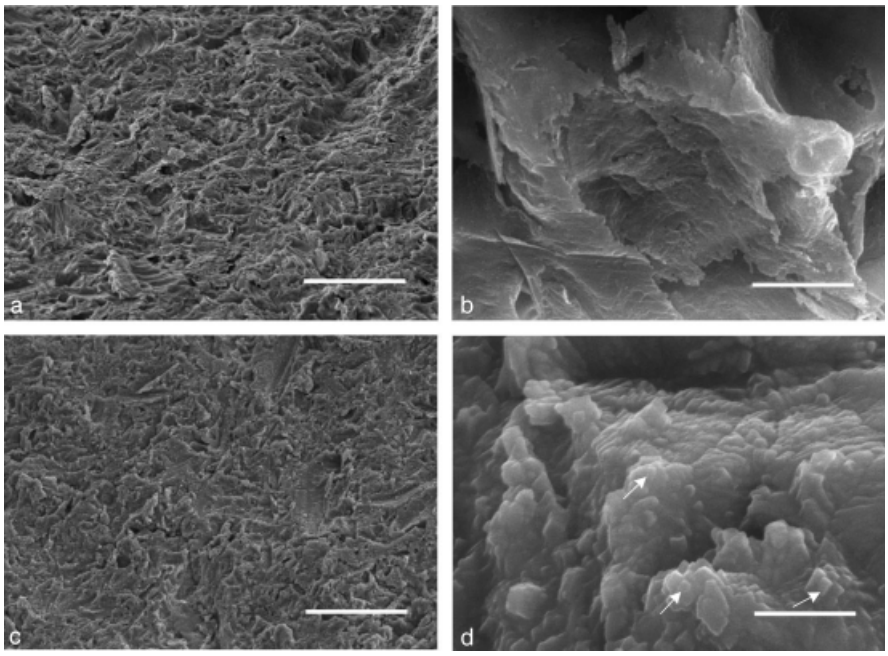

Fig. 1. Scanning electron microscope images of blasted (a, b) and blasted/Ca (c, d) implants at magnifications of × 1000 (a, c) and × 30,000 (b, d). Nanostructure formation (arrows) can be seen on the surface of blasted/Ca implant (d). Scale bars = 30 μm (a, c) and 1 μm (b, d).

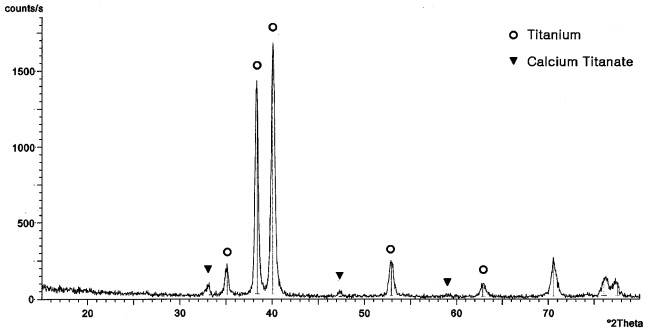

Fig. 2. X-ray diffraction pattern of a blasted/Ca sample.

Removal torque testing

The mean removal torque of the blasted/Ca implants was 42.3 ± 7.9 N cm, significantly higher than that of the blasted implants (35.1 ± 5.6 N cm; $P<0.05$).

Surface analysis of the torqued implants

All torqued, experimental implants exhibited a homogeneous color of deep blue, which was the same as that of original blasted/Ca implants produced by hydrothermal treatment in this study. In SEM observation, a considerable quantity of attached bone was observed on the surfaces of blasted/Ca implants, indicating that fracture had often occurred in the bone (Fig. 4b, c). In contrast, a very limited quantity of attached bone was observed on the surfaces of blasted implants (Fig. 4a) after thorough cleaning in sodium hypochlorite solution. These results indicate that active bone apposition with strong attachment was achieved on the surfaces of blasted/Ca implants in the medullary space, which may be the reason for the

Table 1. **Surface roughness parameters of the implants (Mean ± SD)**

Implant	R_a (μm)	R_q (μm)	R_t (μm)	R_{zDIN} (μm)	S_m (μm)
Blasted	1.7080 ± 0.1401	2.1989 ± 0.2261	11.5765 ± 0.8561	10.1375 ± 1.0031	56.92 ± 9.83
Blasted/Ca	1.3011 ± 0.0720*	1.6797 ± 0.1129*	9.4054 ± 0.0894*	8.2917 ± 1.0439	43.77 ± 2.69

R_a, the arithmetic average of the absolute height values of all points of the profile; R_q, the root mean square of the values of all points of the profile; R_t, the maximum peak-to-valley height of the entire measurement trace; R_{zDIN}, the arithmetic average of the maximum peak to valley height of the roughness, values of five consecutive sampling sections over the filtered profile; S_m, the arithmetic average spacing between the falling flanks of peaks on the mean line.

*significantly different between the two groups at $P<0.05$.

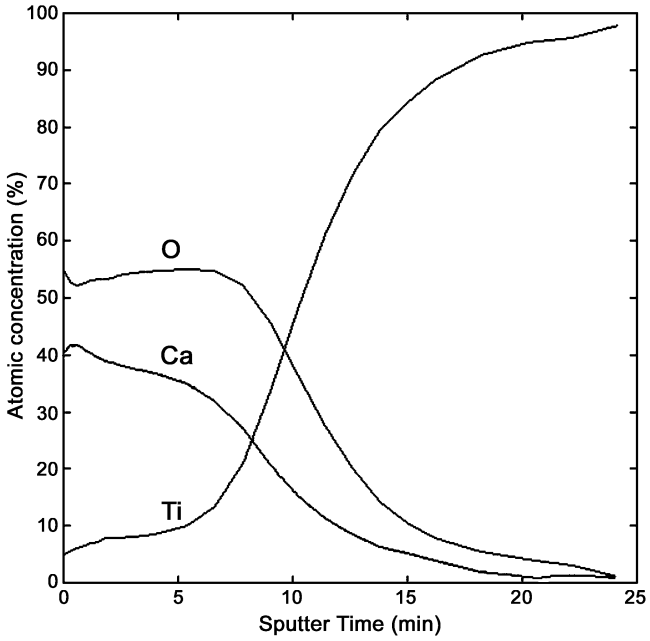

Fig. 3. Auger electron spectroscopy depth profile of a blasted/Ca sample (sputter rate at 23.8 nm/min in SiO_2).

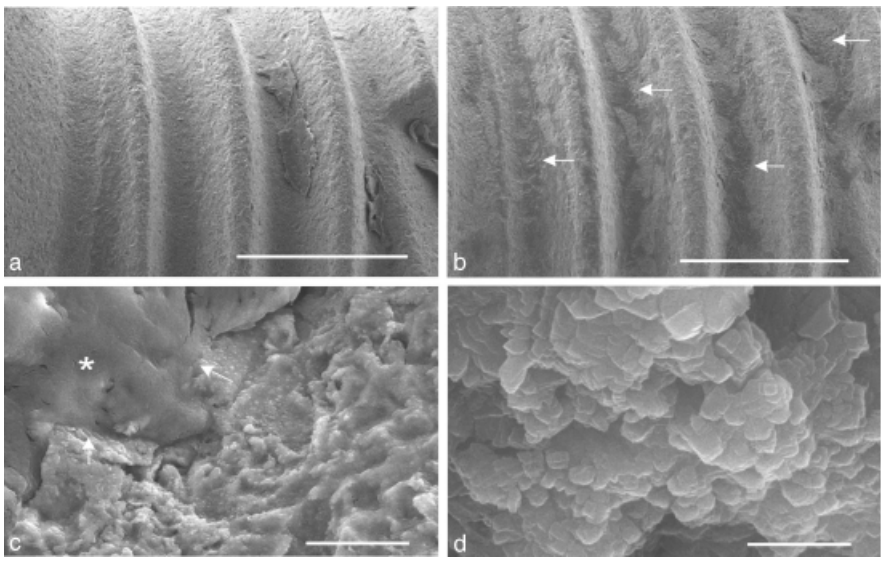

Fig. 4. Scanning electron microscope images of torqued blasted (a) and blasted/Ca (b, c, d) implants at magnifications of × 50 (a, b), × 3000 (c), and × 30,000 (d). Bars equal 1 mm (a, b), 10 μm (c), and 1 μm (d). A considerable amount of attached bone (arrows) can be seen on the surface of blasted/Ca implant (b). The surface of blasted/Ca implant was filled with closely attached bone (asterisk); arrows delineate the borderline between attached bone and implant (c).

higher removal torque value. No signs of surface alteration after removal torque testing were found at either the surfaces of the experimental or the control implants. The torqued blasted/Ca implants showed the original surface nanostructures (Fig. 4d), indicating that $CaTiO_3$ layer has relatively good mechanical properties including coating adhesion and mechanical strength.

Histological evaluation

Six weeks after implantation, all implants in the control and experimental groups were histologically in direct contact with the surrounding bone along their upper threads, with no signs of inflammation or connective tissue interposition at the bone–implant interface in the cortical region (Fig. 5).

The lower threads were in contact with either newly formed bone or marrow tissue (Fig. 6). The blasted/Ca implants showed more active bone formation, and new bone was frequently observed in contact with the lower parts of most implants (in the medullary space). In contrast, very limited bone–implant contact was observed with the blasted implants.

Histomorphometric analysis

The mean BIC% over the total implant length was 29 ± 7.8% for the blasted implants, and 46.9 ± 8.2% for the blasted/Ca implants. In the first three threads, the mean BIC% was 66.1 ± 9.4% for the blasted implants, and 69.4 ± 13.6% for the blasted/Ca implants (Fig. 7). Over the total implant length, the blasted/Ca implants showed a significantly greater mean BIC% compared with the blasted implants ($P<0.01$). There was no statistical difference when comparing the mean BIC% between the two groups in the first three threads ($P>0.05$).

Within the first three threads, the mean bone area percentage was 61.8 ± 5.2% for the blasted implants, and 70.9 ± 7.1% for the blasted/Ca implants (Fig. 7). There was a statistical difference between the two groups ($P<0.05$).

Discussion

In this study, Ca coatings induced active bone apposition on the implant surfaces in the medullary space, which is almost devoid of bony components, and resulted in an increased BIC% over the total length of the implants, while the BIC% of the blasted implants and blasted/Ca implants were similar within the first three threads. These results were the same as those in earlier reported *in vivo* studies in which it was reported that the benefit of a bioactive coating produced by hydroxyapatite plasma spraying is maximized in spongy bone, with enhanced bone apposition not seen in cortical bone (Oonishi et al. 1989; Jansen et al. 1993). Therefore, these results indicate that the use of this type of Ca coating is expected to be most relevant under conditions of poor quality bone, such as in areas of low bone content, where

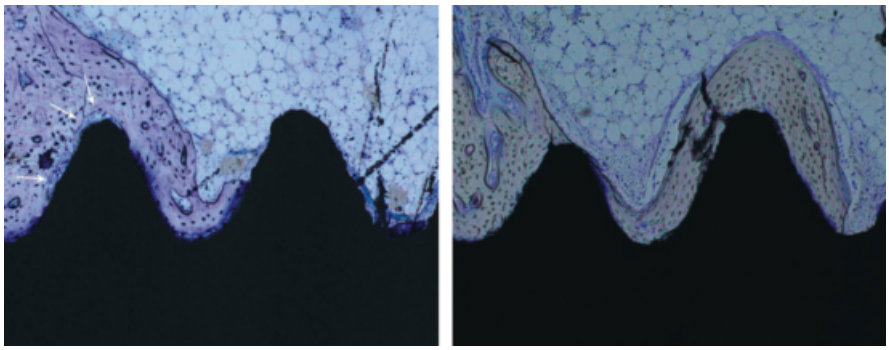

Fig. 5. Histological sections of blasted (left) and blasted/Ca (right) implants at equivalent thread positions below the original cortex. In the blasted implant, incompletely mineralized osteoid matrix (arrow) can be seen in contact with the implant surface. More mature bone can be seen in contact with the blasted/Ca implant. The distance between the threads is 600 μm (stained with toluidine blue).

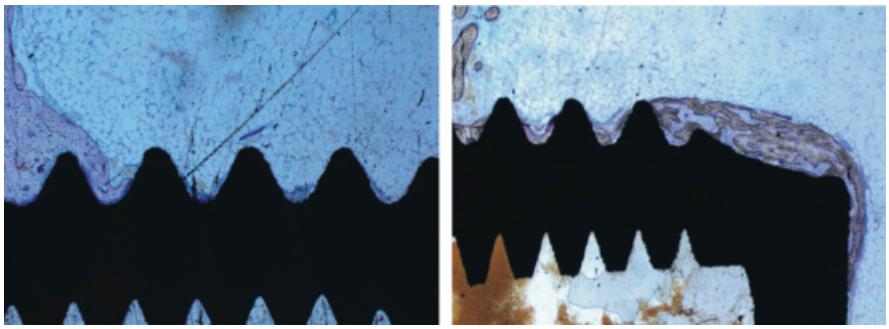

Fig. 6. Histological sections of blasted (left) and blasted/Ca (right) implant 6 weeks after implantation in rabbit tibiae. The blasted/Ca implant shows active bone formation – new bone apposition can be observed on the lower part of the implant, located in the marrow space, which is devoid of surrounding bone. The distance between the threads is 600 μm (stained with toluidine blue).

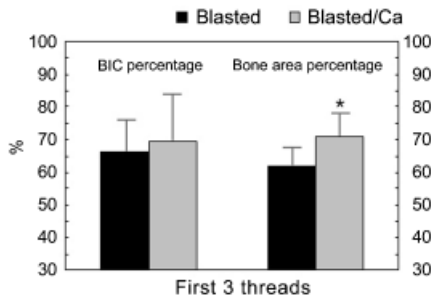

Fig. 7. Mean percentage of the bone-to-implant contact (BIC%) and bone area in the first three threads of implants. The BIC% was not significantly different between the two groups ($P > 0.05$). There was a significant difference in bone area between the two groups ($^*P < 0.05$).

an enhanced bone-healing response is required for successful osseointegration.

It is known that calcium phosphate-coated implants induce faster bone formation. Nevertheless, some drawbacks of plasma spraying associated with the lack of reproducibility in their coatings, such as phase composition, crystallinity, and thickness, have been claimed, which may cause some problems as delamination (however, this is thickness and manufacturer dependent; Hanisch et al. 1997; Burgess et al. 1999; Sun et al. 2001). In contrast to HA plasma-sprayed coatings, this type of Ca coating has several advantages in terms of the mechanical properties of the coating itself. In particular, it does not induce the activation of phagocytic cells by delaminated or dissolved HA particles from coatings, which may impede bone healing and might initiate subsequent cascades of bone resorption (Gottlander et al. 1997; Sabokbar et al. 2001; Sun et al. 2002). However, particulate-induced osteolysis has not been reported as a major finding in dentistry. Hayashi et al. (1994) reported that HA coatings enhance early bone growth on the surface of implants; however, long-term stability depends on bone anchoring to micron-scale surface structure. They suggested that bioactive coatings should be developed that do not obstruct the surface structure of the implant. However, many coating methods providing bioactivity to the metallic implants need a minimum coating thickness before bioactivity is seen, and these coatings obstruct the underlying micron-scale surface structure, a situation that is unavoidable with HA plasma spraying.

The surface morphology of blasted/Ca implants and blasted implants was almost identical at the micron-scale level. The blasted/Ca implants showed slightly smoother surfaces compared with blasted implants ($R_a \approx 1.3$ μm for blasted/Ca implants, 1.7 μm for blasted implants), and therefore the enhanced bone response to the blasted/Ca implants cannot be explained by the effects of micron-scale surface properties. The possible explanation for this finding is that the Ca surface chemistry effectively influenced osseointegration. These results coincide with the findings of other studies, which reported that Ca-incorporated titanium implants showed rapid and strong osseointegration in animal models (Sul et al. 2002; Sul 2003; Jinno et al. 2004).

The blasted/Ca implants showed higher mean peak values for removal torque compared with the blasted implants, which has the slightly decreased value of R_a. The higher removal torque value may be interpreted as an increase in the strength of bony integration at the bone–implant interface. The increased mean peak removal torque value of the blasted/Ca implants is probably due to the surface Ca chemistry, which appeared to improve bone mineralization at the interface, and to the additional effect of the increased BIC% in the marrow space.

The nanostructured Ca coating used in this study may have several advantages in enhancing the bone response around endosseous titanium implants.

The surface has more abundant Ca compared with that reported in other studies (Ca ≈ 40% at the outer surface). Sul (2003) reported a maximum of 11% of Ca incorporation into a Ti oxide matrix using micro-arc oxidation. It is believed that integrin function is critically dependent on the concentration of divalent cations. It may be possible that the increased amount of Ca may facilitate integrin-mediated attachment of bone-forming cells through enhanced ligand binding of the integrin receptor (Ajroud et al. 2004).

Nayab et al. (2005) reported that Ca implantation in Ti significantly affected the spreading of the MG-63 cells, both qualitatively and quantitatively. They indicated that an increased dose of Ca enhanced the network of fibrillar processes between cells and toward the Ti surface. Several studies have suggested that an increased Ca composition in the outer oxide layer increases the adsorption of polyanionic proteins, including proteoglycans, onto Ti surfaces by ionic bonding at physiologic pH, which subsequently increases cell adhesion and provides nucleation sites for mineral formation (Lindhe et al. 1989; Ellingsen 1991; Klinger et al. 1997). The increased amount of Ca in the Ti oxide layer of the Ti implants may be the possible reason for the enhanced bone responses seen in this study.

The coating preserves micron-scaled surface properties, including microroughness and topography. Most methods for providing bioactivity to metallic implants need a minimum coating thickness to show bioactivity (Wolke et al. 1999). These coatings obscure the underlying micron-scale surface properties produced by surface pretreatment such as blasting and/or etching and related to biomechanical interlocking. The Ca-coating method used in this study produces the surface layer by a dissolution–reprecipitation mechanism, not as a simple additive coating (Eckert et al. 1996). This may be the possible reason for the unique surface characteristics of this coating layer, with preservation of the microarchitecture. This Ca-coating method may be considered a promising approach of providing bioactivity to endosseous Ti implants with microroughened surfaces, replacing plasma-sprayed HA coatings.

The coating layer has a surface nanostructure. Although there are no proven advantages for a surface nanostructure in enhancing implant stabilization in clinical use, several *in vitro* studies reported that nanotopography has significant biological effects on cultured osteogenic cells. It was reported that the nanoscale surface structure enhanced osteoblast adhesion and subsequent cellular function due to increased present optimal sites for osteoblast adhesion on the surface (Elias et al. 2000; Webster & Ejiofo 2004). The enhanced early deposition of bone sialoprotein and osteopontin, containing RGD sequences, on nanotextured Ti surfaces was reported in osteogenic cell culture (de Oliveira & Nanci 2004). It may be considered that nanoscale surface structures may provide a potential approach for enhancing peri-implant bone responses in clinical use. However, more research is needed to provide a definite mechanism and confirm the results *in vivo*.

Although it is not clear which surface property – Ca chemistry or nanoscale surface structure – more greatly affected the enhanced quality and quantity of peri-implant bone formation around the blasted/Ca implants in this study, this coating layer positively increased the osteoconductivity of blasted Ti implants. The nanoscale surface structure also increases the surface area, which subsequently increases the area of the Ca coating exposed to the biological environment and increases the reactivity of the implant surface, influencing the initial protein adsorption, subsequent bone cell adhesion, and mineral formation. This may be another reason for the improved peri-implant bone response, as measured by biomechanical tests and histomorphometric evaluation.

Surface modification with a nanostructured Ca coating could thus prove to be an effective tool for improving bone formation *in vivo* and the clinical efficacy of bioinert endosseous titanium implants.

In summary, the use of bioconductive Ca coatings is expected to have advantages in suboptimal situations involving poor-quality bone, such as in areas of low bone content, where an enhanced bone response is required for successful osseointegration. Moreover, it is suggested that the use of nanostructured Ca-coated surfaces may have a synergic effect in enhancing osseointegration of blasted Ti implants due to the micron-scale surface properties and biologically active surface chemistry. However, further studies are needed to better understand the effects of this nanostructured Ca-incorporated surface on bone responses.

要旨

目的：本研究の目的は、家兎の脛骨においてブラスト Ti インプラント表面上のナノ構造のカルシウム・コーティングが、インプラント周囲の骨形成に及ぼす影響を調べることであった。

材料と方法：ねじ式インプラント（直径３．７５ｍｍ、長さ６．０ｍｍ）にハイドロキシアパタイト（HA）を吹きつけて粗造にした（対照：ブラスト・インプラント）。次にインプラントをカルシウム含有溶液中で２４時間熱水処理を行い、Ti 表面に Ca が取り込まれるようにした（実験インプラント：ブラスト／Ca インプラント）。Ca コーティングの前後に、走査電子顕微鏡と尖筆側面計によって表面特性を調べた。インプラント４２本（対照２１本、実験２１本）を７羽のニュージーランド白色家兎の脛骨近位に埋入した。術後６週間後に抜去トルク試験と組織形態計測を行い、ナノ構造の Ca コーティングがインプラント周囲骨の治癒反応に及ぼす影響を評価した。

結果：Ca コーティングは、ミクロン・レベルの吹き付けによる粗造表面の特性を変化させなかった。組織像では、ブラスト／Ca インプラントにおいて髄腔で活発な骨添加が観察された。ブラスト・インプラントに比べ、ブラスト／Ca インプラントはインプラント全長にわたって骨とインプラントの接触が有意に増加しており（$p < 0.01$）、平均抜去トルク値も有意に高かった（$p < 0.05$）。

考察と結論：ナノ構造の Ca 取り込み表面は、HA ブラスト Ti インプラント周囲の骨治癒反応を有意に促進した。ナノ構造の Ca コーティング表面は、ミクロン単位の表面特性と生物学的に活性な表面化学特性を有するため、ブラスト Ti インプラントの骨性結合を促進する上で相乗効果があると結論しうる。

References

Adell, R., Eriksson, B., Lekholm, U., Brånemark, P.I. & Jemt, T. (1990) Long-term follow-up study of osseointegrated implants in the treatment of totally edentulous jaws. *International Journal of Oral & Maxillofacial Implants* **5**: 347–359.

Ajroud, K., Sugimori, T., Goldmann, W.H., Fathallah, D.M., Xiong, J.P. & Arnaout, M.A. (2004) Binding affinity of metal ions to the CD11b A-domain is regulated by integrin activation and ligands. *Journal of Biological Chemistry* **279**: 25483–25488.

Albrektsson, T. (1998) Hydroxyapatite-coated implants: a case against their use. *Journal of Oral and Maxillofacial Surgery* **56**: 1312–1326.

Burgess, A.V., Story, B.J., La, D., Wagner, W.R. & LeGeros, J.P. (1999) Highly crystalline MP-1™ hydroxyapatite coating Part I: *in vitro* character-

ization and comparison to other plasma-sprayed hydroxyapatite coatings. *Clinical Oral Implants Research* **10**: 245–256.

Caulier, H., van der Waerden, J.P., Wolke, J.G., Kalk, W., Naert, I. & Jansen, J.A. (1997) Histological and histomorphometrical evaluation of the application of screw designed calcium phosphate (Ca-P)-coated implants in the cancellous maxillary bone of the goat. *Journal of Biomedical Materials Research* **35**: 19–30.

Cochran, D.L., Buser, D., ten Bruggenkate, C.M., Weingart, D., Taylor, T.M., Bernard, J., Peters, F. & Simpson, J.P. (2002) The use of reduced healing times on ITI® implants with a sandblasted and acid-etched (SLA) surface: early results from clinical trials on ITI® SLA implants. *Clinical Oral Implants Research* **13**: 144–153.

Davies, J.E. (1998) Mechanism of endosseous integration. *International Journal of Prosthodontics* **11**: 391–401.

de Oliveira, R.T. & Nanci, A. (2004) Nanotexturing of titanium-based surfaces upregulates expression of bone sialoprotein and osteopontin by cultured osteogenic cells. *Biomaterials* **25**: 403–413.

Eckert, J.O., Hung-Houston, C.C., Gerten, B.L., Lencka, M.M. & Riman, R.E. (1996) Kinetics and mechanism of hydrothermal synthesis of barium titanate. *Journal of American Ceramic Society* **79**: 2929–2939.

Elias, K.E., Price, R.L., Haberstroh, K.M. & Webster, T.J. (2000) Enhanced functions of osteoblasts on nanometer diameter carbon fibers. *Biomaterials* **23**: 3279–3287.

Ellingsen, J.E. (1991) A study on the mechanism of protein adsorption to TiO_2. *Biomaterials* **12**: 593–596.

Fujishiro, Y., Sato, N., Uchida, S. & Sato, T. (1998) Coating of $CaTiO_3$ on titanium substrates by hydrothermal reactions using calcium-ethylene diamine tetra acetic acid chelate. *Journal of Materials Science: Materials in Medicine* **9**: 363–367.

Glauser, R., Ruhstaller, P., Windisch, S., Zembic, A., Lundgren, A., Gottlow, J. & Hammerle, C.H. (2005) Immediate occlusal loading of Branemark System TiUnite implants placed predominantly in soft bone: 4-year results of a prospective clinical study. *Clinical Implants Dentistry & Related Research* **7**: S52–59.

Gottlander, M., Johansson, C. & Albrektsson, T. (1997) Short- and long-term animal studies with a plasma-sprayed calcium phosphate-coated implant. *Clinical Oral Implants Research* **8**: 345–351.

Hanisch, O., Cortella, C.A., Boskovic, M.M., James, R.A., Slots, J. & Wikesjo, U.M. (1997) Experimental peri-implant tissue breakdown around hydroxyapatite-coated implants. *Journal of Periodontology* **68**: 59–66.

Hayashi, K., Inadome, T., Tsumura, H., Nakashima, Y. & Sugioka, Y. (1994) Effect of surface roughness of hydroxyapatite-coated titanium on the bone – implant interface shear strength. *Biomaterials* **15**: 1187–1191.

Jaffin, R.A. & Berman, C.L. (1991) The excessive loss of Brånemark fixtures in type IV bone: a 5-year analysis. *Journal of Periodontology* **62**: 2–4.

Jansen, J.A., van der Waerden, J.P. & Wolke, J.G. (1993) Histologic investigation of the biologic behavior of different hydroxyapatite plasma-sprayed coatings in rabbits. *Journal of Biomedical Materials Research* **27**: 603–610.

Jinno, T., Kirk, S.K., Morita, S. & Goldberg, V.M. (2004) Effects of calcium ion implantation on osseointegration of surface blasted titanium alloy femoral implants in a canine total hip arthroplasty model. *Journal of Arthroplasty* **19**: 102–109.

Johansson, C.B., Han, C.H., Wennerberg, A. & Albrektsson, T. (1998) A quantitative comparison of machined commercially pure titanium and titanium-aluminium-vanadium implants in rabbit bone. *International Journal of Oral & Maxillofacial Implants* **13**: 315–321.

Kaciulis, S., Mattogno, G., Napoli, A., Bemporad, E., Ferrari, F., Montenero, A. & Gnappi, G. (1998) Surface analysis of biocompatible coatings on titanium. *Journal of Electron Spectroscopy and Related Phenomena* **95**: 61–69.

Karabuda, C., Sandalli, P., Yalcin, S., Steflik, D.E. & Parr, G.R. (1999) Histologic and histomorphometric comparison of immediately placed HA-coated and titanium plasma-sprayed implants: a pilot study in dogs. *International Journal of Oral & Maxillofacial Implants* **14**: 510–515.

Khang, W., Feldman, S., Hawley, C.E. & Gunsolley, J. (2001) A multi-center study comparing dual acid-etched and machined-surfaced implants in various bone qualities. *Journal of Periodontology* **72**: 1384–1390.

Klinger, A., Steinberg, D., Kohavi, D. & Sela, M.N. (1997) Mechanism of adsorption of human albumin to titanium *in vitro*. *Journal of Biomedical Materials Research* **36**: 387–392.

Lindhe, A., Lussi, A. & Crenshaw, M.A. (1989) Mineral induction by immobilized polyanionic proteins. *Calcified Tissue International* **44**: 286–295.

Lossdorfer, S., Schwartz, Z., Wang, L., Lohmann, C.H., Turner, J.D., Wieland, M., Cochran, D.L. & Boyan, B.D. (2004) Microrough implant surface topographies increase osteogenesis by reducing osteoclast formation and activity. *Journal of Biomedical Materials Research A* **70**: 361–369.

Manso, M., Langlet, M. & Martinez-Duart, J.M. (2003) Testing sol–gel $CaTiO_3$ coatings for biomedical applications. *Materials Science and Engineering C* **23**: 447–450.

Morscher, E.W., Hefti, A. & Aebi, U. (1998) Severe osteolysis after third-body wear due to hydroxyapatite particles from acetabular cup coating. *Journal of Bone and Joint Surgery. British Volume* **80**: 267–272.

Nayab, S.N., Jones, F.H. & Olsen, I. (2005) Effects of calcium ion implantation on human bone cell interaction with titanium. *Biomaterials* **26**: 4717–4727.

Oonishi, H., Yamamoto, M., Ishimaru, H., Tsuji, E., Kushitami, S., Aono, M. & Ukon, Y. (1989) The effect of hydroxyapatite coatings on bone growth into porous titanium alloys implants. *Journal of Bone and Joint Surgery* **71**: 213–216.

Sabokbar, A., Pandey, R., Diaz, J., Quinn, J.M., Murray, D.W. & Athanasou, N.A. (2001) Hydroxyapatite particles are capable of inducing osteoclast formation. *Journal of Materials Science. Materials in Medicine* **12**: 659–664.

Stach, R.M. & Kohles, S.S. (2003) A meta-analysis examining the clinical survivability of machined-surfaced and Osseotite implants in poor-quality bone. *Implant Dentistry* **12**: 87–96.

Sul, Y.T. (2003) The significance of the surface properties of oxidized titanium to the bone response: special emphasis on potential biochemical bonding of oxidized titanium implant. *Biomaterials* **24**: 3893–3907.

Sul, Y.T., Johansson, C.B. & Albrektsson, T. (2002) Oxidized titanium screws coated with calcium ions and their performance in rabbit bone. *International Journal of Oral & Maxillofacial Implants* **17**: 625–634.

Sun, L., Berndt, C.C., Gross, K.A. & Kucuk, A. (2001) Material fundamentals and clinical performance of plasma-sprayed hydroxyapatite coatings: a review. *Journal of Biomedical Materials Research* **58**: 570–592.

Sun, L., Berndt, C.C., Khor, K.A., Cheang, H.N. & Gross, K.A. (2002) Surface characteristics and dissolution behavior of plasma-sprayed hydroxyapatite coating. *Journal of Biomedical Materials Research* **62**: 228–236.

Szmukler-Moncler, S., Perrin, D., Bernard, J.P. & Pointaire, P. (2004a) Biological properties of acid etched titanium surface. Effect of sandblasting on bone anchorage. *Journal of Biomedical Materials Research B, Applied Biomaterials* **15**: 149–159.

Szmukler-Moncler, S., Testori, T. & Bernard, J.P. (2004b) Etched implants: a comparative surface analysis of four implant systems. *Journal of Biomedical Materials Research B, Applied Biomaterials* **69**: 46–57.

Trisi, P., Rao, W. & Rebaudi, A. (1999) A histometric comparison of smooth and rough titanium implants in human low-density jawbone. *International Journal of Oral & Maxillofacial Implants* **14**: 689–698.

van Steenberghe, D., Lekholm, U., Bolender, C., Folmer, T., Henry, P., Herrmann, I., Higuchi, K., Laney, W., Lindhe, U. & Astrand, P. (1990) The applicability of osseointegrated oral implants in the rehabilitation of partial edentulism: a prospective multicenter study on 558 fixtures. *International Journal of Oral & Maxillofacial Implants* **5**: 272–281.

Webster, T.J. & Ejiofo, J.U. (2004) Increased osteoblast adhesion on nanophase metals: Ti, Ti6Al4 V, and CoCrMo. *Biomaterials* **25**: 4731–4739.

Webster, T.J., Ergun, C., Doremus, R.H. & Lanford, W.A. (2003) Increased osteoblast adhesion on titanium-coated hydroxyapatite that forms $CaTiO_3$. *Journal of Biomedical Materials Research A* **67**: 975–980.

Wennerberg, A., Hallgren, C., Johansson, C. & Daneelli, S. (1998) A histomorphometric evaluation of screw-shaped implants each prepared with two surface roughness. *Clinical Oral Implants Research* **9**: 11–19.

Wolke, J.G.C., Vercaigne, S., van der Warden, J.P., Schaeken, H.G. & Jansen, J.A. (1999) *In vivo* dissolution behavior of various RF magnetron sputtered Ca–P coatings on roughened titanium implants. *Bioceramics* **12**: 487–490.

Yoshimura, M., Urushihara, W., Yashima, M. & Kakihana, M. (1995) $CaTiO_3$ coating on TiAl by hydrothermal-electrochemical technique. *Intermetallics* **3**: 125–128.